Biophysical Journal Volume 73 November 1997 2476–2488

Interplay Between Sodium and Calcium Dynamics in Granule Cell Presynaptic Terminals

Wade G. Regehr
Department of Neurobiology, Harvard Medical School, Boston, Massachusetts 02115 USA

ABSTRACT Fluorescent indicators were used to detect stimulus-evoked changes in presynaptic levels of intracellular sodium (Na_i) and calcium (Ca_i) in granule cell parallel fibers in brain slices from rat cerebellum. Ca_i increased during stimulation, and three exponentials were needed to approximate its return to prestimulus levels. Ca_i decayed to ~10% of peak levels with $\tau \sim 100$ ms, to ~1% of peak values with $\tau \sim 6$ s, and then returned to prestimulus levels with $\tau \sim 1$–2 min. After stimulation, Na_i accumulated in two phases; one rapid, the other continuing for several hundred milliseconds. The return of Na_i to prestimulus levels was well approximated by a double exponential decay with time constants of 6–17 s and 2–3 min. Manipulations that prevented calcium entry eliminated both the slow component of sodium entry and the rapid component of Na_i decay. Reductions of extracellular sodium slowed the rapid phase of Ca_i decay. These Ca_i and Na_i transients were well described by a model in which the plasma membrane of presynaptic boutons contained both a sodium/calcium exchanger and a calcium ATPase (Ca-ATPase). According to this model, immediately after stimulation the sodium/calcium exchanger removes calcium from the terminal more rapidly than does the Ca-ATPase. Eventually, the large concomitant sodium influx brings the exchanger into steady-state, leaving only the Ca-ATPase to remove calcium. This perturbs the equilibrium of the sodium/calcium exchanger, which opposes the Ca-ATPase, leading to a slow return of Ca_i and Na_i to resting levels.

INTRODUCTION

High firing rates in neurons lead to a buildup of free calcium (Ca_i) in their presynaptic terminals. These increases in Ca_i enhance synaptic strength (Atluri and Regehr, 1996; Delaney and Tank, 1994; Delaney et al., 1989; Regehr et al., 1994; Swandulla et al., 1991; Zucker et al., 1991). The factors that control the decay of Ca_i, and thereby influence the time course of Ca_i-dependent synaptic enhancement, are not fully understood.

Studies of pinched-off nerve terminals (synaptosomes) have revealed important features of presynaptic calcium regulation (Blaustein and Santiago, 1977; Blaustein and Oborn, 1975; Duarte et al., 1991; Fontana and Blaustein, 1993; Fontana et al., 1995; Gill et al., 1981; Sanchez-Armass and Blaustein, 1987). There are two primary systems for removing calcium from synaptosomes, the sodium/calcium exchanger and the calcium ATPase (Ca-ATPase). The sodium/calcium exchanger is electrogenic and exchanges 3 sodium ions for one calcium ion. Depending on the membrane potential, and the intracellular and extracellular concentrations of Na^+ and Ca^{2+}, this exchange mechanism can either bring Ca^{2+} into the cell or remove Ca^{2+} from the cell. The sodium/calcium exchanger has a high capacity for Ca^{2+} removal, but a low-affinity for Ca^{2+} (Allen et al., 1989). In contrast, the plasmalemma calcium ATPase has a low capacity for calcium removal, a higher Ca^{2+} affinity, and is powered by ATP (Carafoli et al., 1996).

The sodium/calcium exchanger and the Ca-ATPase are also thought to be the dominant means of calcium extrusion in intact presynaptic terminals of the mammalian CNS (Fujii et al., 1996; Luther et al., 1992; Reuter and Porzig, 1995; Bouron and Reuter, 1996). Stimulation of presynaptic fibers can produce large increases in presynaptic Ca_i. In parallel fibers, single stimuli increase Ca_i by several hundred nanomolar (Atluri and Regehr, 1996). After stimulation Ca_i returns to resting levels with a complex time course. Ca_i decays to 10% of peak levels in hundreds of milliseconds, but then decays more slowly (Atluri and Regehr, 1996). This slow component of decay becomes more prominent as the number of stimulus pulses is increased. It has been difficult to establish the roles of the sodium/calcium exchanger and the plasma membrane Ca-ATPase in calcium extrusion, because selective pharmacological agents are not available to inhibit these extrusion mechanisms.

Here I investigate the determinants of presynaptic calcium levels by optically detecting presynaptic Na_i and Ca_i transients produced by stimulus trains. Measurements were made from intact presynaptic boutons from cerebeller granule cells in rat brain slices. Na_i and Ca_i levels were found to be intimately linked. During stimulation, Na_i and Ca_i both rose quickly in presynaptic terminals. Ca_i decayed to ~10% of peak levels within a few hundred milliseconds, and as it did so Na_i continued to increase. This second phase of sodium accumulation was found to be coupled to calcium efflux. On longer time scales, there were similarities in the time course of sodium and calcium decay. These results are consistent with an interplay between Na_i and Ca_i levels mediated by the sodium/calcium exchanger. A model is

Received for publication 22 May 1997 and in final form 29 July 1997.

Address reprint requests to Wade G. Regehr, Department of Neurobiology, Harvard Medical School, 220 Longwood Ave., Boston, MA 02115. Tel.:617-432-0435; Fax: 617-734-7557; E-mail: wregehr@warren.med.harvard.edu.

0006-3495/97/11/2476/13 $2.00

presented that accounts for important features of the Na_i and Ca_i transients.

METHODS

Transverse slices (300 μm thick) were cut from the cerebellar vermis of 14- to 24-day-old Sprague-Dawley rats as described previously (Llano et al., 1991; Mintz et al., 1995). The slices were allowed to recover at 30°C for 1 h before use and experiments were conducted at 20–24°C. The external solution consisted of (in mM): 125 NaCl, 2.5 KCl, 2 $CaCl_2$, 1 $MgCl_2$, 26 $NaHCO_3$, 1.25 NaH_2PO_4, 25 glucose, and 0.02 bicuculline, bubbled with 95% O_2 and 5% CO_2.

Detection of presynaptic Na_i and Ca_i transients

Parallel fibers were labeled with a high-pressure stream of mag-fura-5, fura-2, magnesium orange, or sodium-binding benzofuran isophthalate (SBFI) (Delbono and Stefani, 1993; Grynkiewicz et al., 1985; Minta and Tsien, 1989; Zhao et al., 1996) using techniques developed previously (Regehr and Atluri, 1995; Regehr and Tank, 1991). Loading times were 5 to 10 min for the calcium-sensitive indicators and 30 to 60 min for SBFI. After waiting 2 h for dye to diffuse and equilibrate within the fibers, an electrode was placed in the labeled band to stimulate parallel fibers. The resulting fluorescence transients were detected from an 80-μm spot located 100–150 μm from the stimulus electrode and 300–600 μm from the fill site.

The preparation was illuminated with a 150 Watt Xenon bulb (model XBO 150W/CR OFR, Osram, Germany), which was gated with a shutter (model VS25S27M1-21, Vincent Associates, Rochester, NY). For the indicators SBFI, fura-2, and mag-fura-5 the filter set consisted of a 380DF15 excitation filter, a 425DRLP dichroic mirror, and a GG455 emission filter. For magnesium orange a 540DF15 excitation filter, a 560DLP dichroic mirror, and a 570OG emission filter were used. All optical filters were from Omega Optical (Brattleboro, VT). Decreases in fluorescence correspond to increases in ionic levels for mag-fura-5, fura-2, and SBFI. Fluorescence transients for these indicators have been inverted for clarity.

For experiments in which ionic levels were monitored for <20 s (Figs. 1–5 and 9), the preparation was illuminated continuously. For longer duration experiments, such as those shown in Figs. 7 and 8, the preparation was illuminated for 100 ms every second for 20 s prior to stimulation, then continuously illuminated from 300 ms before stimulation to 3 s after stimulation. For the next 2–5 min the preparation was illuminated for 100 ms every second. $\Delta F/F$ values were determined for each of the illumination periods. This enabled me to follow the relatively rapid transients that occurred during and immediately after stimulation, as well as the slow decays of ionic levels on very long time scales, without significantly bleaching the indicator (as would have occurred with continuous illumination). A photodiode was used to detect fluorescence. All records were corrected for bleaching as described previously (Regehr and Atluri, 1995). Signals were filtered at 200 Hz with an 8-pole Bessel filter (Frequency Devices, Haverhill, MA) and sampled at 2 kHz with the Instrutech ITC 16 interface (Great Neck, NY) using Pulse Control software (Herrington and Bookman, 1995).

Limitations of Na_i and Ca_i detection

This method of detecting Na_i and Ca_i had a number of limitations. 1) Measurements of ionic levels were from parallel fibers, which are heavily dominated by presynaptic terminals but also include small axonal segments (Palay and Chan-Palay, 1974). Thus, simulations based on single compartment models may not apply on rapid time scales, and this may contribute to differences in the time courses of Na_i accumulation and Ca_i decay (see below). 2) It is not possible to use a single calcium indicator to measure Ca_i on all of the time scales owing to limitations of the indicators (see Results). Therefore, low affinity dyes were used to measure calcium levels that were sufficiently large to saturate high affinity dyes (such as fura-2), and high affinity dyes were used to measure the small calcium levels present at long times after stimulation. 3) Quantification of Na_i levels in these experiments using SBFI was not possible. The ratio method cannot be applied since the fluoresence signal arises from stimulated and unstimulated fibers. In addition, Na_i increases produced by long stimulus trains may be sufficiently large to partially saturate the response of SBFI. Although similar problems associated with the fluorescence measurement of calcium levels in these fibers were overcome (Feller et al., 1996; Regehr and Atluri, 1995), there is not a sufficient variety of sodium indicators available to take a similar approach to sodium quantification. Saturation of SBFI would result in a slowing of the fluorescence transients relative to actual changes in Na_i and a sublinear relationship between $\Delta F/F$ and Na_i. However, when few stimulus pulses are used, the increases in Na_i are sufficiently small that for SBFI the relationship between $\Delta F/F$ and Na_i is linear, and SBFI provides a good measure of rate of Na_i decay.

Simulations of Na_i and Ca_i transients

Simulations of Na_i and Ca_i levels were calculated with Euler integration using time steps of 100 μs (see Table I). These simulations were based on a number of assumptions:

1. Spatial ionic gradients were ignored. This assumption is likely to hold at long times after stimulation, when diffusion would have largely dissipated spatial gradients, and it appears to be valid for crayfish presynaptic terminals and chromaffin cells for such conditions (Neher and Augustine, 1992; Tank et al., 1995). It may not apply for several hundred milliseconds after stimulation, if, for example, the sources and sinks of calcium and sodium are located in different regions of the parallel fibers.
2. Mitochondria (Rizzuto et al., 1992, 1994) and intracellular stores targeted by ryanodine and IP_3 (Ehrlich et al., 1994) were ignored. Several studies indicate that internal stores participate in calcium regulation in some presynaptic terminals (Blaustein, 1988; Peng, 1996; Tang and Zucker, 1997). Thus far we find no experimental evidence for their participation at this synapse (Sabatini and Regehr, 1995); this is similar to the properties of calcium transients in goldfish bipolar cells (Kobayashi and Tachibana, 1995). Simulations suggest that intracellular stores are not required to explain the sodium and calcium dynamics in parallel fibers. Further experimentation will be required, however, to determine whether these stores contribute to calcium regulation in these presynaptic boutons for some experimental conditions.
3. Resting Na_i levels (Na_{rest}) and Ca_i levels (Ca_{rest}) were taken to be 10 mM and 40 nM, respectively. Although Ca_{rest} is notoriously difficult to measure, 40 nM is consistent with estimates of Ca_{rest}. The value of Na_{rest} corresponds to a reversal potential of 70 mV and is within the range of reported values of Na_{rest} (Harootunian et al., 1989; Levi et al., 1994; Satoh et al., 1991; Rose and Ransom, 1997).
4. Each action potential triggered calcium entry through voltage-gated calcium channels that was sufficient to increase free calcium by ΔCa_i and free sodium by ΔNa_i. The default value used for ΔCa_i had been determined experimentally (Regehr and Atluri, 1995).
5. The presynaptic bouton was assumed to contain a low affinity calcium buffer at a concentration [B] with a dissociation constant, K_B. It is assumed that on the time scale of these simulations calcium is in equilibrium with the buffer and that, where the total concentration of calcium in the bouton (Ca_T) is equal to the sum of the free calcium concentration (Ca_i) and the concentration of calcium bound to buffer, [CaB] (i.e., $Ca_T = Ca_i + [CaB]$). Although the calcium buffer capacity within the granule cell presynaptic boutons is not known, the buffer capacities for chromaffin cells, crayfish nerve terminals, the calyx of Held, and hair cells have been measured, and range from 40 to 4000 (Helmchen et al., 1997; Neher and Augustine, 1992; Roberts et al., 1990; Tank et al., 1995; Tucker and Fettiplace, 1996). The default values used in the simulations correspond to $[B]/K_B = 250$. Based on

TABLE 1 Default values of parameters used in simulations

Description	Variable Name	Default Value
External calcium concentration	Ca_e	2 mM
Resting internal calcium	Ca_{rest}	40 nM
Maximum calcium pump velocity	R_{Camax}	0.5 mM s^{-1}
Half-maximal value for the pump	K_P	200 nM
Calcium change per spike	ΔCa_T	62.5 μM
Concentration of calcium buffer	[B]	5 mM
Dissociation constant of calcium buffer	K_B	20 μM
External sodium concentration	Na_e	150 mM
Resting internal sodium	Na_{rest}	10 mM
Sodium change per spike	ΔNa_i	80 μM
Membrane potential	V	−70 mV
Sodium/calcium exchanger constant	$K_{Na/Ca}$	3×10^5 M^{-3} s^{-1}

observed properties of calcium transients produced by trains, the buffer in parallel fiber terminals has $K_B > 5$ μM (Regehr and Atluri, 1995).

6. The rate of extrusion by the Ca-ATPase was approximated by the Michaelis-Menten formulation:

$$\left(\frac{dCa_T}{dt}\right)_{pump} = -\frac{V_{max}Ca_i}{K_p + Ca_i}. \quad (1)$$

7. The simple scheme given below was used to approximate the extrusion rates of the sodium/calcium exchanger (Mullins, 1977). The changes in Ca_i and Na_i are given by:

$$\left(\frac{dCa_T}{dt}\right)_{Na/Ca} = K_{Na/Ca}(Na_i^3Ca_e e^{V/2kT} - Na_e^3Ca_i e^{-V/2kT}) \quad (2)$$

$$\left(\frac{dNa_i}{dt}\right)_{Na/Ca} = -3\left(\frac{dCa_T}{dt}\right)_{Na/Ca} \approx -\frac{3[B]}{K_B}\left(\frac{dCa_i}{dt}\right)_{Na/Ca} \quad (3)$$

Although more sophisticated models have been advanced for the cardiac sodium/calcium exchanger (Hilgemann, 1988; Hilgemann et al., 1992; Matsuoka and Hilgemann, 1992), this model captured the fundamental features of the exchanger required to explain the observed sodium and calcium transients: 3 sodium ions are exchanged for 1 calcium ion and the reversal potential of the exchanger is given by

$$V_m = V_{NaCa} = -kT\left(3\ln\left(\frac{Na_i}{Na_e}\right) - \ln\left(\frac{Ca_i}{Ca_e}\right)\right). \quad (4)$$

There is no net flux of ions through the exchanger when the membrane potential equals the reversal potential of the exchanger ($V = V_{NaCa}$).

8. For simplicity, sodium extrusion mechanisms other than the sodium/calcium exchanger were ignored. Measurements of Na_i suggest that such extrusion mechanisms do not greatly affect Na_i levels in the first 30 s after stimulation.

RESULTS

Fluorescent indicators were used to detect changes in intracellular levels of free sodium (Na_i) and free calcium (Ca_i) within parallel fibers. Na_i was monitored with the indicator SBFI, which has a dissociation constant for sodium of 20 mM (Minta and Tsien, 1989). Ca_i was monitored with the indicators mag-fura-5, fura-2, and magnesium orange, which have dissociation constants for calcium of 31 μM, 100–200 nM, and 43 μM, respectively (Grynkiewicz et al., 1985; Zhao et al., 1996). These fluorophores were introduced into parallel fibers by locally loading a membrane-permeant form of the indicator using a procedure that has been described previously. After allowing 2–3 h for the indicator to diffuse within the parallel fibers, the pattern of labeling is such that in the molecular layer, far from the loading site, the only structures containing the indicator are the parallel fibers. Using an electrode placed in the molecular layer to stimulate parallel fibers, fluorescence changes from an 80-μm diameter spot were monitored with a photodiode or a photomultiplier tube. These measurements represent an aggregate measure of the fluorescence changes in many parallel fibers. Anatomical studies suggest that the volume of the parallel fibers is ~85–90% presynaptic terminal, with thin axonal segments accounting for the remaining volume (Palay and Chan-Palay, 1974).

Na_i and Ca_i dynamics immediately after stimulation

Stimulation of parallel fibers with high frequency trains evoked large presynaptic calcium transients that were detected with mag-fura-5 (Fig. 1 *A*). Previous studies have shown that these fluorescence transients result from calcium entering parallel fibers through voltage-gated calcium channels and that single action potentials increase Ca_i by 200 to 300 nM (Atluri and Regehr, 1996). This allows us to estimate Ca_i, and in Fig. 1 *A* the scale bar corresponds to ~500 nM. Low affinity indicators, such as mag-fura-5, also provide a good measure of the time course of Ca_i decay in the first several seconds after stimulation (Atluri and Regehr, 1996; Regehr and Atluri, 1995). After such stimulus trains, Ca_i decays to 10% of peak levels within a second.

The rates of Ca_i decay from the same initial level are compared in the inset of Fig. 1 *A* for transients produced by different duration stimulation. The fluorescence transients have been shifted to allow a comparison of the calcium decay from the same level of Ca_i. Increasing the number of stimuli slowed the return of Ca_i to resting levels. This dependence of the decay rate on the number of stimulus pulses is inconsistent with simple models of presynaptic calcium dynamics, which predict that calcium should decay with the same time course from a given value of Ca_i, independent of the number of impulses in the train (see Fig. 10 *A inset*).

High frequency stimulus trains also produced SBFI fluorescence transients (Fig. 1 *B*), consistent with an increase in presynaptic Na_i levels. Though it is difficult to estimate the amplitude of Na_i changes with SBFI (see Methods), these signals provide important qualitative information about the sources of sodium and sodium extrusion mechanisms. Unexpectedly, they suggest that Na_i continues to increase after the termination of stimulation, when Ca_i has already begun to decay.

Experiments such as those shown in Fig. 1 also suggest that the time course of the Na_i increase is comparable to the time course of the rapid decay of Ca_i. Approximating the

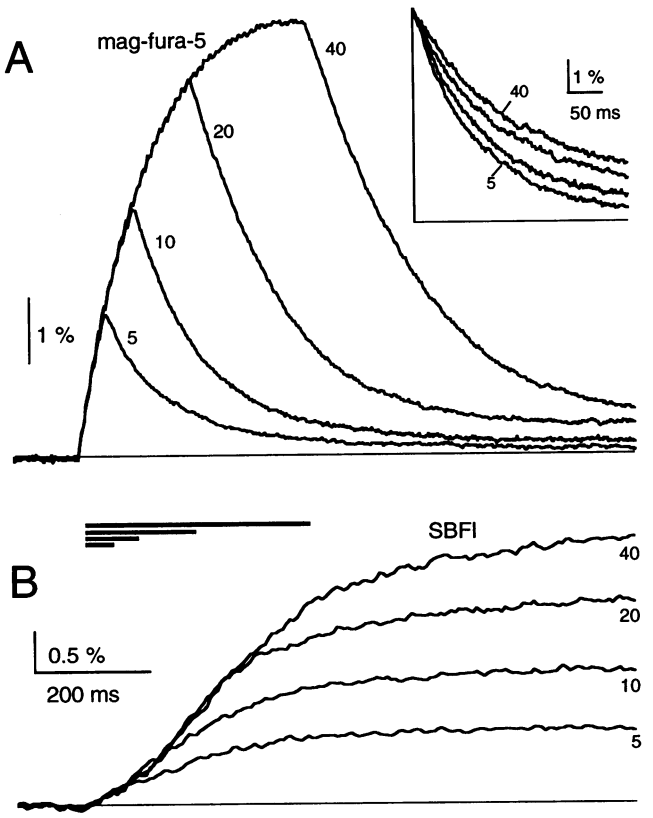

FIGURE 1 Stimulus-evoked presynaptic $\Delta F/F$ transients of sodium and calcium indicators. Fluorescence changes produced by stimulation of parallel fibers with 100-Hz trains of 5, 10, 20, and 40 stimuli for the calcium-sensitive indicator mag-fura-5 (*A*) and for the sodium indicator SBFI (*B*). The stimulus periods for the four trains are indicated by bold lines. Inset in (*A*) shows the mag-fura-5 fluorescence traces shifted in time to facilitate the comparison of the time course of $\Delta F/F$ decay from a given value of $\Delta F/F$ for each of the four stimulus trains. The traces in (*A*) and (*B*) are from different experiments.

$\Delta F/F$ signals produced by stimulating with 5 pulses at 100 Hz with an exponential over the range of 30 to 500 ms poststimulus, mag-fura-5 $\Delta F/F$ signals decayed with a time constant of 70–110 ms (n = 10), and SBFI fluorescence increased with a time constant of 193 ± 10 ms (n = 10). This similarity in the time course of Ca_i decay and Na_i accumulation suggested that the levels of these ions are linked.

Na_i and Ca_i dynamics were also compared within the same set of presynaptic terminals. A number of indicators were tested and magnesium orange was found to be the best suited to these studies (Zhao et al., 1996). It has a low affinity for calcium and excitation and emission spectra that do not overlap with those of SBFI. Parallel fibers were labeled with both magnesium orange and SBFI, and in alternate trials measurements were performed with either the sodium-sensitive or the calcium-sensitive indicator (Fig. 2). Again, Ca_i decayed with a time course similar to, but somewhat faster than, the slow phase of sodium accumulation (80 ± 2 ms compared to 200 ± 20 ms, n = 5).

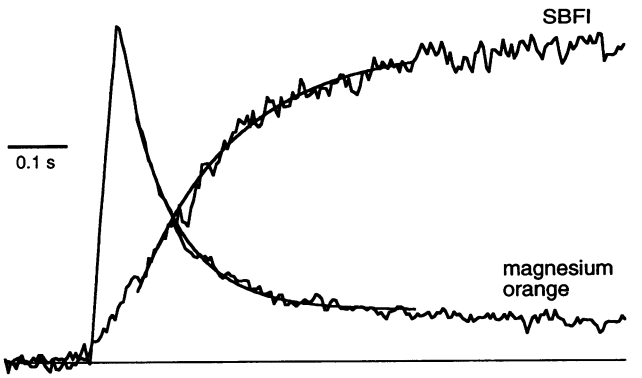

FIGURE 2 $\Delta F/F$ changes from a fiber tract loaded with both SBFI the calcium-sensitive indicator magnesium orange. Fluorescence changes produced by five stimuli at 100 Hz. Traces are normalized to facilitate the comparison of the time course of $\Delta F/F$ changes. Peak $\Delta F/F$ changes were 1.8% for magnesium orange and 1.4% for SBFI. Traces are the average of 10 trials for SBFI and four trials for magnesium orange. Fits are exponential over the indicated ranges with time constants of 170 ms for the buildup of Na_i and 90 ms for the decay of Ca_i.

Characterization of the sodium transients

Several pharmacological manipulations were used to characterize the SBFI $\Delta F/F$ transients. Although only the parallel fibers should have been loaded with SBFI, it was important to verify that the fluorescence changes did not arise from inadvertent labeling of postsynaptic elements. The coapplication of 10 μM CNQX and 50 μM AP5 did not significantly affect the SBFI fluorescence transients produced by 5-pulse 100 Hz trains (a reduction of 11 ± 9%, n = 4). In addition, 400 nM TTX reversibly eliminated SBFI fluorescence transients (peak values were reduced to 1 ± 1%, n = 3). Together these results indicate that in these recordings postsynaptic elements do not contribute to SBFI $\Delta F/F$ signals and that the signals require a propagating action potential.

As shown in Fig. 3, cadmium, which blocks voltage-gated calcium channels, was a useful tool for dissecting the SBFI fluorescence transients into two components. In control conditions, the SBFI fluorescence transients produced by 100-Hz trains of 1 to 4 stimuli appeared to consist of two kinetically separable components; one increased abruptly after stimulation and the other increased more slowly. Cadmium did not affect the faster component (Fig. 3 *B*), whereas it eliminated the slow component of Na_i accumulation (Fig. 3 *C*). The differences in the kinetics of these two components are clearly shown in Fig. 3 *D*. The cadmium-sensitive component accounted for 74 ± 8% (n = 14) of the sodium accumulation.

To quantitatively test the calcium-dependence of sodium entry I examined the effect of several manipulations of calcium entry on Na_i accumulation. One hundred-Hz trains with 5 stimulus pulses produced $\Delta F/F$ signals with good signal-to-noise ratios that were sufficiently small to avoid saturation of the SBFI response. A previous study showed that cadmium reduced calcium influx in parallel fibers with

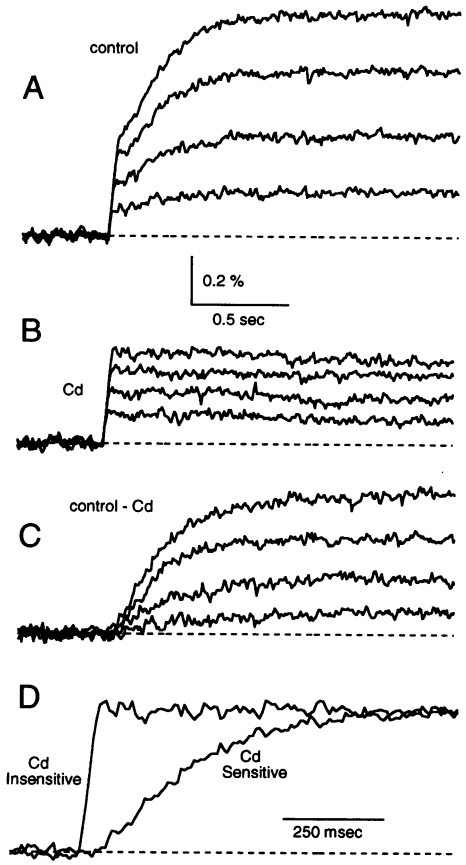

FIGURE 3 The effects of cadmium on changes in SBFI fluorescence produced by brief trains. SBFI fluorescence changes evoked by trains of one to four stimuli at 100 Hz are shown for control solution (*A*) and in the presence of 100 μM cadmium (*B*). The cadmium-insensitive component (*C*) was determined by subtracting the traces in *B* from the traces in *A*. (*D*) The normalized responses produced by trains of four stimuli at 100 Hz from *B* and *C*. Each trace is the average of five trials.

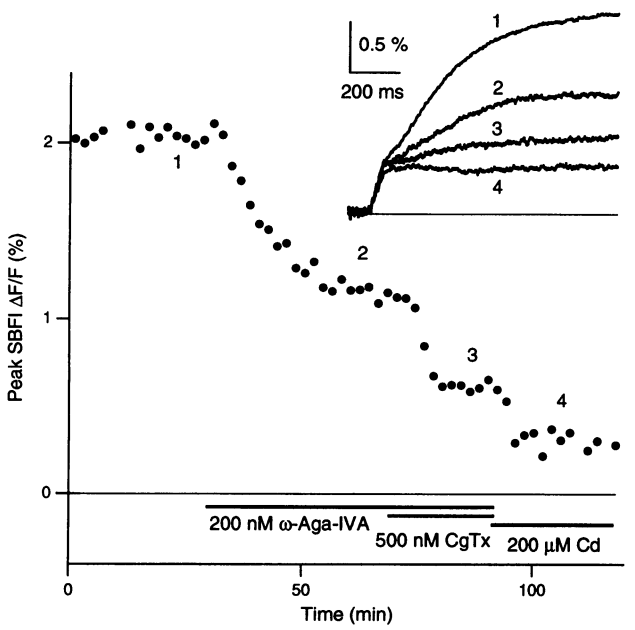

FIGURE 4 The effects of reduced presynaptic calcium entry on presynaptic sodium transients. The effects of extracellular cadmium or reducing extracellular calcium on SBFI fluorescence changes produced by five stimuli at 100 Hz. Insets show average SBFI fluorescence transients for various conditions.

an EC_{50} of 6 μM, and that the dependence of calcium influx on extracellular calcium (Ca_e) was well approximated by a function of the form $Ca_e/(Ca_e + 3\ mM)$ (Mintz et al., 1995). As shown in Fig. 4, the slow component of the SBFI $\Delta F/F$ signals was reduced by changing from control solution (2 mM Ca_e) to either 1 mM Ca_e or 0.5 mM Ca_e, as well as by adding 5 μM cadmium to the control solution.

The effects of two peptide toxins on SBFI fluorescence transients were also examined. ω-Conotoxin GVIA, which targets N-type calcium channels (Fujita et al., 1993; Williams et al., 1992), has previously been shown to block 27.0 ± 1.7% of calcium influx at this synapse, while ω-Aga-IVA, which targets P/Q-type calcium channels (Mintz et al., 1992), blocks 50.1 ± 1.8% of the calcium influx (Mintz et al., 1995). At the concentrations employed here these toxins block non-overlapping fractions of calcium accumulation in parallel fibers without affecting sodium channels or presynaptic action potentials (Mintz et al., 1995; Regehr and Mintz, 1994). As shown in Fig. 5, ω-Aga-IVA reduced the amplitude of the slow component of the $\Delta F/F$ signals to 54 ± 6% of control values ($n = 4$) and a coapplication of ω-Aga-IVA and ω-conotoxin GVIA further reduced the amplitude of the signals to 22 ± 6% of control ($n = 4$).

It was clear from these experiments that decreasing the amplitude of the calcium accumulations reduced the size of the slow component of the SBFI $\Delta F/F$ signal without affecting the rapid component. Fig. 6 compares the relative sizes of the slow component of sodium accumulation and the amplitude of calcium accumulation for these different conditions. These points are well approximated by the line, which corresponds to a one-to-one relationship between the amplitude of these two quantities.

Taken together, the results described thus far suggest that the slow component of sodium accumulation is a consequence of calcium extrusion from the cytoplasm of parallel fibers. The rapid component of sodium accumulation is likely a consequence of sodium entry through TTX-sensitive sodium channels that open during the presynaptic action potential. For stimulus trains of 4 or 5 pulses at 100 Hz the calcium-dependent slow component is 2.9 ± 0.3 ($n = 14$) times as large as the rapid component of SBFI $\Delta F/F$ signal. Thus, for such stimulus trains, a great deal more sodium enters parallel fibers as a consequence of a calcium-dependent mechanism than directly through voltage-gated sodium channels.

Na_i and Ca_i dynamics on long time scales

Na_i and Ca_i dynamics were also examined on longer time scales. Ca_i was monitored with fura-2, which is more sen-

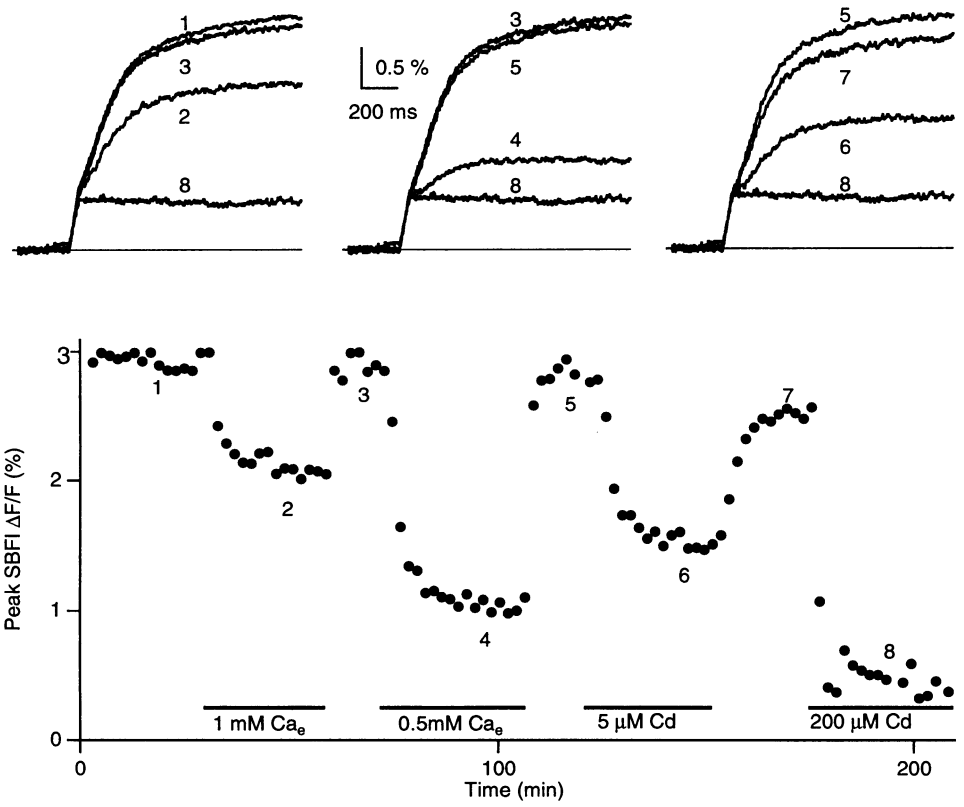

FIGURE 5 The effects of reduced presynaptic calcium entry on presynaptic sodium transients. The effects of the calcium channel antagonists ω-Aga-IVA and ω-conotoxin GVIA on SBFI $\Delta F/F$ changes produced by 100 Hz trains of five stimuli. Insets show average SBFI fluorescence transients for various conditions.

sitive to calcium and less sensitive to small changes in intracellular magnesium levels than magnesium orange or mag-fura-5. Fura-2 fluorescence transients produced by 100-Hz trains are shown from 1 to 100 s after tetanic stimulation (Fig. 7, *A* and *C*). The 1-s interval immediately after tetanic stimulation is not displayed. During this period Ca_i is sufficiently high to saturate the response of fura-2. After 1 s Ca_i had already decayed to ~10% of peak levels (Fig. 1 *A*). Ca_i then decays to ~1% of peak values with τ_{Ca2} of 6 to 7 s. Although it is difficult to reliably measure slower components of decay, it appears that Ca_i ultimately returns to prestimulus levels with τ_{Ca3} of 60 to 120 s. The inset in Fig. 7 *A* shows that the slow decay of Ca_i from a given level gets progressively slower as the number of pulses in the stimulus trains is increased (as demonstrated previously for the more rapid decay phase of calcium in the inset of Fig. 1 *A*).

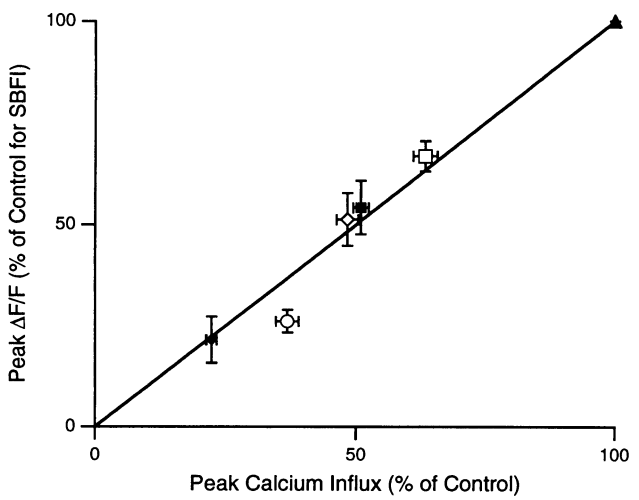

FIGURE 6 A comparison of the effects of manipulations of calcium entry on the magnitude of sodium entry. A comparison of the effects of 1 mM Ca_e (*open square*), 0.5 mM Ca_e (*open circle*), 5 μM cadmium (*solid square*), 200 nM ω-Aga-IVA (*open diamond*), and a coapplication of ω-Aga-IVA and ω-conotoxin GVIA (*solid diamond*), on the amplitude of the slow component of the sodium accumulation (as determined in Figs. 4 and 5) and on the amplitude of presynaptic calcium influx [as determined previously (Mintz et al., 1995)].

The decay of presynaptic Na_i was remarkably slow. As shown in Fig. 7, *B–D*, following stimulation with 100-Hz trains of 5 to 40 pulses, SBFI $\Delta F/F$ signals were well approximated by a double exponential decay, with τ_{Na1} 5–17 s and τ_{Na2} of 120 s to 180 s. The slow component of Na_i decay was prominent, and 20 s after stimulating with five stimuli Na_i was still at 46% of peak levels.

The similarity of τ_{Ca2} to τ_{Na1} and of τ_{Ca3} to τ_{Na2} suggested that Na_i and Ca_i dynamics are also coupled on these longer time scales. I tested this by blocking voltage-gated calcium channels with cadmium. As shown in Fig. 8, this had a major impact on the Na_i decay. In addition to blocking most of the calcium entry into the presynaptic terminals, and eliminating the slowly rising component of sodium accumulation, the decay of SBFI fluorescence changes became extremely slow. The return to resting levels could be ap-

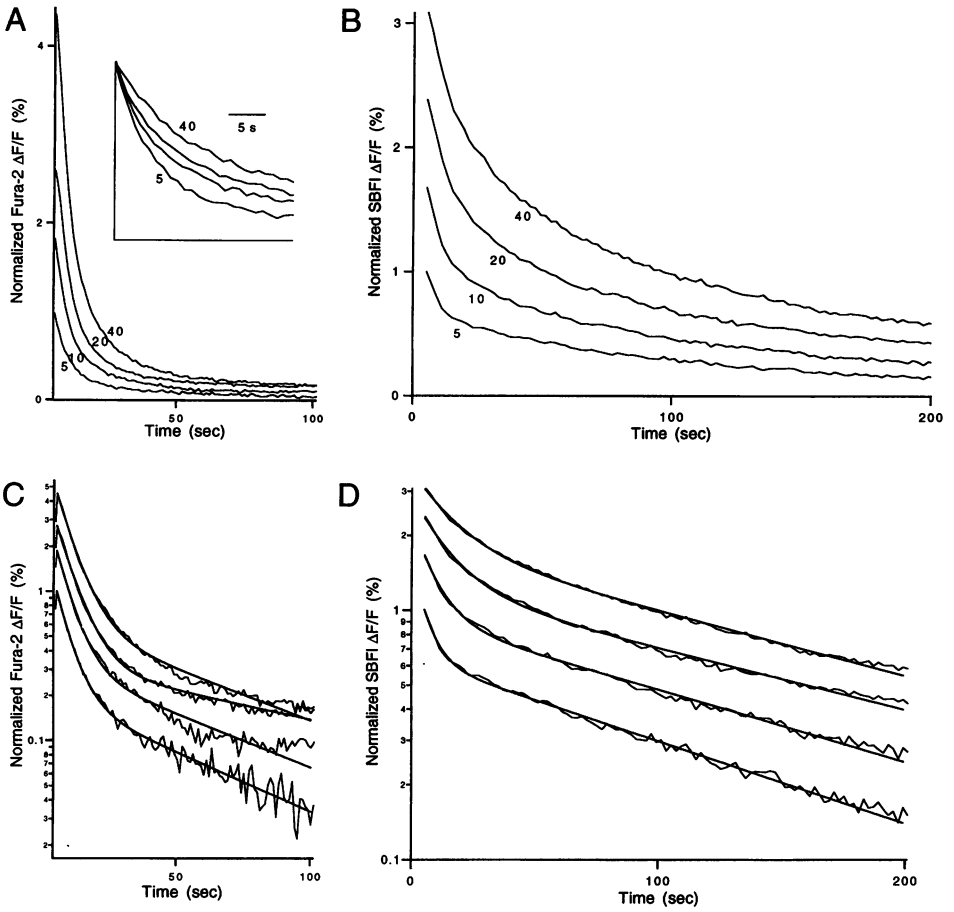

FIGURE 7 The decay of Ca_i and Na_i at long times after stimulus trains. Linear (*A* and *B*) and semilogarithmic (*C* and *D*) plots of fura-2 (*A* and *C*) and SBFI fluorescence (*B* and *D*) produced by 100-Hz stimulus trains of 5, 10, 20, and 40 pulses. Each trace is normalized to the $\Delta F/F$ signal produced by five pulses at 1 s after the end of stimulation. Traces are the average of five experiments. Fits in (*C*) and (*D*) are to functions of the form $ae^{(-t/\tau_1)} + be^{-(t/\tau_2)}$ where the parameters $\{\tau_1, \tau_2\}$ are {5.6, 56}, {5.9, 63}, {6.9, 112}, and {6.7, 63} for fura-2, and {5.9, 133}, {8.9, 151}, {14.5, 175}, and {16.7, 169} for SBFI, for 5, 10, 20, and 40 stimuli, respectively.

proximated by a single exponential decay with a time constant of more than 3 min. The more rapid component of Na_i decay that was apparent in control conditions (τ_{Na1} 5 to 17 s), was eliminated by cadmium.

The dependence of calcium extrusion on extracellular sodium

The dependence of Na_i transients on calcium entry suggested the involvement of the sodium/calcium exchanger. I tested this possibility by examining the effects of lowering external sodium (Na_e) on the calcium transients (27 mM, compared to 152 mM Na_e for standard external saline). In these experiments, although lithium substitutes for sodium in the voltage-gated sodium channels, there are certain to be minor effects on fiber excitability and presynaptic waveform. This makes interpretation of changes in the amplitude of $\Delta F/F$ signals difficult to interpret. These ionic substitution experiments are much more informative with regard to rates of extrusion. Lithium does not substitute for sodium in the sodium/calcium exchanger, and low Na_e should reduce the rate of calcium extrusion via the sodium/calcium exchanger (Kobayashi and Tachibana, 1995; Reuter and Porzig, 1995). In low Na_e solution the most rapid phase of calcium extrusion was slowed (Fig. 9 *A*), but the time course of the subsequent Ca_i decay was unaffected (Fig. 9 *B*). These findings are consistent with the sodium/calcium exchanger playing an important role in the initial phase (the first several hundred milliseconds) of calcium removal, but not during subsequent calcium extrusion.

Simulations of sodium and calcium transients

The observed interplay between Na_i and Ca_i, and the dependence of the rapid decay of Ca_i on external sodium levels, established the importance of the sodium/calcium exchanger in presynaptic calcium regulation. Without selective pharmacological agents to inhibit the exchanger (Wettwer et al., 1992) or the plasmalemma calcium ATPase, I examined the relative contribution of these extrusion mechanisms by simulating presynaptic Na_i and Ca_i levels. These simulations were based on a single compartment model of the presynaptic terminal, with sodium and calcium entering through voltage-gated channels and calcium within the terminal binding to buffer. Calcium was removed via a calcium ATPase and/or the sodium/calcium exchanger. These simulations were based on a number of simplifying assumptions that are described in the Methods.

Fig. 10, *A–C* shows simulated Ca_i transients for different extrusion conditions. Each panel shows simulated responses to 100-Hz stimulus trains. Simulations with a Ca-ATPase as the sole means of calcium extrusion for trains of 10, 20, 30,

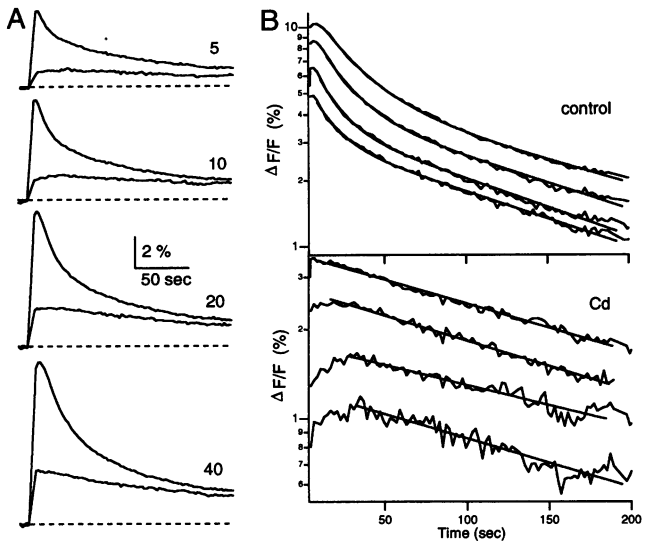

FIGURE 8 The effect of cadmium on SBFI fluorescence transients at long times after stimulus trains. (*A*) SBFI fluorescence transients measured in control solution and in the presence of 100 μM cadmium for 100-Hz stimulus trains consisting of the indicated number of pulses. (*B*) Semilogarithmic plots of the fluorescence transients in *A*. Note the different scales for the different conditions.

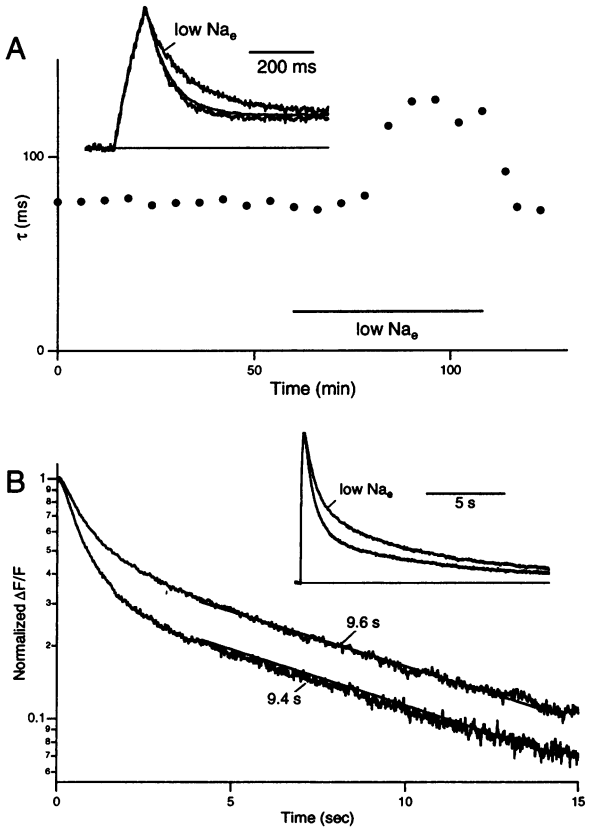

FIGURE 9 The effect of low external sodium on presynaptic calcium transients. (*A*) The time constant of the rapid component of presynaptic calcium decay measured with mag-fura-5. Inset shows normalized average mag-fura-5 $\Delta F/F$ transients produced by 10 pulses at 100 Hz before, during, and after application of low external sodium. The time constants were determined by an exponential fit over the range 0–500 ms after the end of stimulation. (*B*) Semilog plot of fura-2 $\Delta F/F$ changes in standard and in low external sodium solutions produced by 200-ms 100-Hz stimulation. Fits shown are to single exponential decays of the form $ae^{-t/\tau}$, where $\{a, t\}$ is $\{0.35, 9.4\}$ for control conditions and $\{0.46, 9.6\}$ for low external sodium. Inset shows a standard plot of the same data.

and 40 stimuli result in the family of curves shown in Fig. 10 *A*. As shown in the inset, for these conditions the decays of Ca_i from 500 nM to rest had an identical time course for these different trains. This is inconsistent with the experimentally observed transients (Fig. 1 *A* and 7 *A insets*). Such differences between simulated and observed calcium transients remained for a broad range of Ca-ATPase densities and affinities.

Simulations that included only the sodium/calcium exchanger were also clearly deficient (Fig. 10 *B*). In these simulations, calcium decayed rapidly to ~10% of peak levels, but never returned to resting levels (Fig. 10 *D*). One attractive feature of these simulations was that the Ca_i decay rate depended on the number of pulses in the stimulus train, as is apparent when examining the decay of calcium from 500 nM (*inset*).

Simulations that included both the sodium/calcium exchanger and the Ca-ATPase provided a much better approximation to the experimentally observed transients. When both extrusion mechanisms were present (Fig. 10 *C*) Ca_i eventually returned to resting levels (Fig. 10 *D*).

It is revealing to examine in greater detail the situation when the sodium/calcium exchanger is the sole means of extrusion. For greater ease in interpretation these simulations, and the rest of the simulations in the paper, assume that the initial increases in Na_i and Ca_i occur instantaneously. After this initial increase, Ca_i decays to low levels within a second (Fig. 11, *A* and *D*). While it does so, Na_i continues to increase (Fig. 11 *B*) as a consequence of the sodium/calcium exchanger (Fig. 11 *C*), which brings 3 sodium ions into the cell for each calcium ion removed. Eventually Na_i and Ca_i plateau at elevated levels and never return to resting levels.

A plot of the Ca_i versus the Na_i for these simulations provides insight into what is happening for these conditions (Fig. 11 *E*). As a result of influx through voltage-gated channels, Na_i and Ca_i abruptly increase from rest (indicated by the triangle) to the levels indicated by the solid dots. The size of this abrupt change is proportional to the number of pulses in the train. At this point the sodium/calcium exchanger is far from equilibrium, and it removes calcium from the bouton in exchange for sodium. From Eq. 3 it can be shown that Na_i and Ca_i levels follow the line,

$$Ca_i = -\frac{K_B}{3[B]}(Na_i - Na_1) + Ca_1, \qquad (5)$$

where Ca_1 and Na_1 are Ca_i and Na_i immediately after stimulation. This exchange of calcium for sodium continues

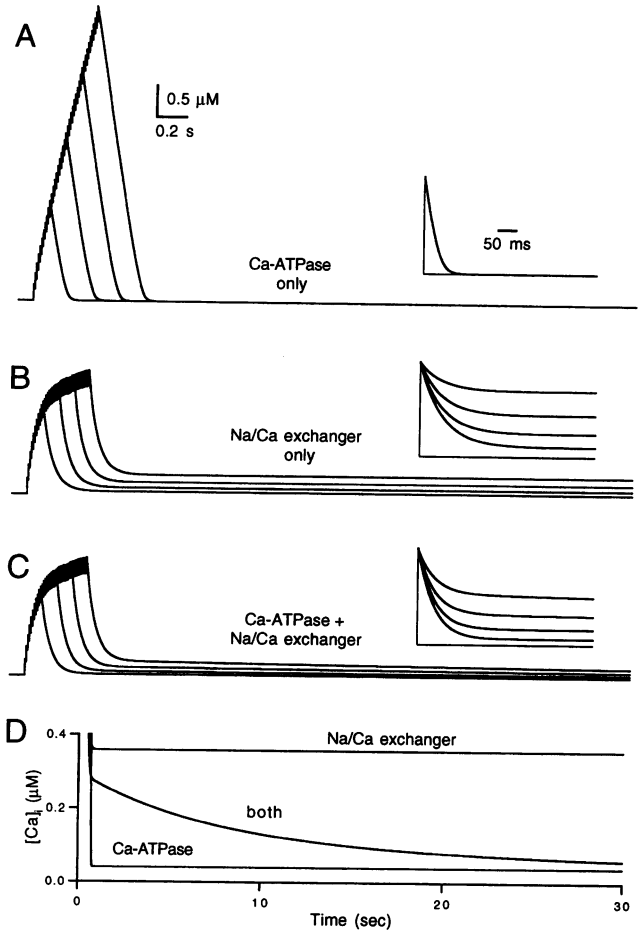

FIGURE 10 Simulations of calcium transients using different extrusion mechanisms. Simulations of Ca_i for 100-Hz trains produced by 10, 20, 30, and 40 pulses assuming that calcium was removed by the Ca-ATPase alone (*A*), the sodium/calcium exchanger alone (*B*), and both the Ca-ATPase and the sodium/calcium exchanger (*C*). The scale bar applies to all three sets of simulation in (*A*) to (*C*). In the insets associated with (*A*) to (*C*) the traces are realigned to compare the time course of calcium decay for each family of simulated calcium transients. Each trace is from 500 nM to Ca_{rest} (40 nM). The scale bar in the inset of (*A*) applies to all of the insets. (*D*) Ca_i transients produced by 40 pulses for the three different conditions of calcium extrusion. Default parameters were used in simulations except in (*A*) the density of the Ca-ATPase was 5 mM s^{-1} and there was no sodium/calcium exchanger present, and in (*B*) there was no Ca-ATPase present.

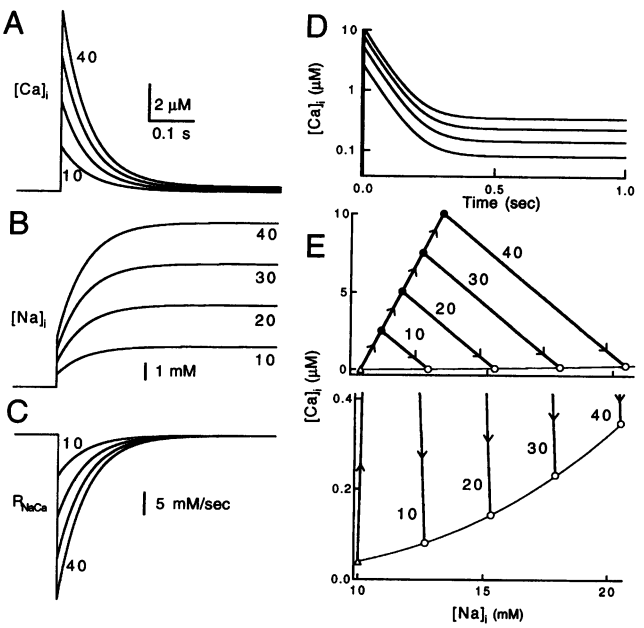

FIGURE 11 Simulated Ca_i and Na_i dynamics with only the sodium/calcium exchanger present. Ca_i transients (*A*), Na_i transients (*B*), and the rate of sodium/calciumexchange (*C*) for 10, 20, 30, and 40 pulses in which, for simplicity, it was assumed that the changes in Ca_i and Na_i were instantaneous. In (*D*) the Ca_i decays are replotted on a semilog plot to more clearly show that these calcium transients plateau at an elevated level. In (*E*) the Ca_i values from (*A*) are plotted against the corresponding values for Na_i from (*B*). Resting levels are indicated by the open triangle, levels immediately after stimulation are indicated by the closed circles, and steady-state levels are indicated by the open circles. The curve passing through the resting and steady-state levels is given by Eq. 5 (*thick line*). Simulations used default values for the parameters except that there was no sodium/calcium exchanger present.

until the sodium/calcium exchanger is in equilibrium, a condition that is given by

$$Ca_i = Na_i^3 \frac{Ca_e}{Na_e^3} e^{V/kT} = \alpha Na_i^3. \quad (6)$$

Equation 6 follows from Eq. 4 and because Ca_e, Na_e, and V are taken to be constants following stimulation, α is a constant. If $Ca_i > \alpha Na_i^3$, then the sodium/calcium exchanger removes calcium from the cell and elevates Na_i, if $Ca_i < \alpha Na_i^3$, the sodium/calcium exchanger extrudes sodium and brings calcium into the cell. When the sodium/calcium exchanger is the only extrusion mechanism present, the Na_i and Ca_i levels will remain elevated at the intersection of the line given by Eq. 5 and the curve given by Eq. 6. The points of intersection for trains of 10 to 40 stimuli are indicated by the open circles in Fig. 11 *E*. It should be noted that when only the sodium/calcium exchanger is present, the calcium decay is well approximated by an exponential with a time constant of decay given by,

$$\tau = \frac{([B]/K_B)}{R_{Na/Ca}} \quad (7)$$

where $R_{Na/Ca} = K_{Na/Ca} Na_e^3 e^{-V/2kT}$. This expression is similar to the expression for the decay of calcium when the only extrusion mechanism is a calcium pump (Neher and Augustine, 1992; Tank et al., 1995).

The effects of the inclusion of the CaATPase as well as the sodium/calcium exchanger are examined in more detail in the simulations of Fig. 12. The Ca-ATPase has little effect on Ca_i and Na_i transients at short times (Fig. 12, *A* and *B*). This is not surprising because when Ca_i is high the rate of extrusion via the low affinity sodium/calcium exchanger is much greater than for the high affinity Ca-ATPase (compare Fig. 12 *C* to Fig. 12 *D*). The sodium/calcium exchanger adjusts Ca_i and Na_i, and rapidly brings

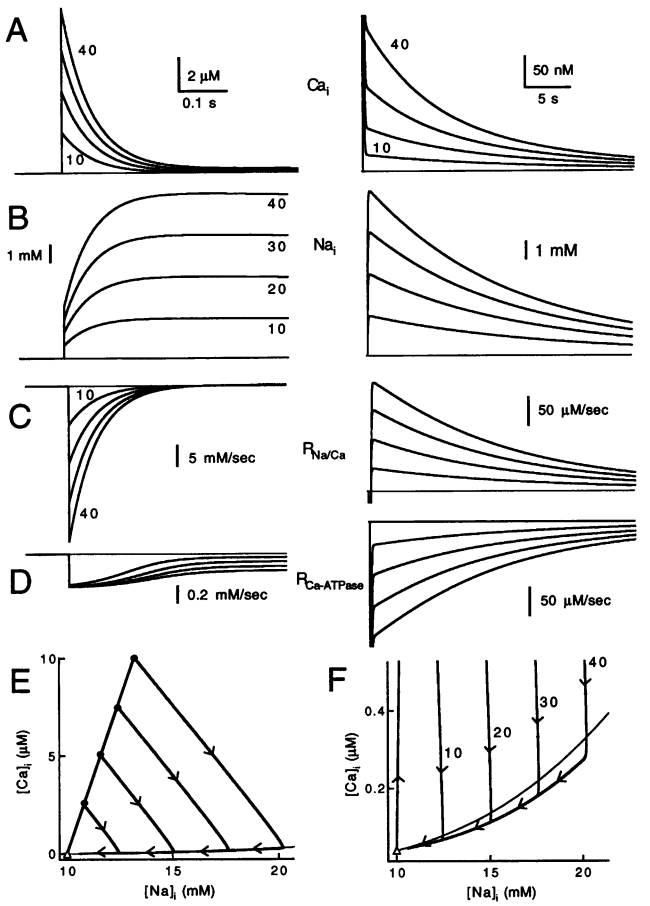

FIGURE 12 Simulations of Ca_i and Na_i dynamics with both the sodium/calcium exchanger and the Ca-ATPase present. Ca_i transients (*A*), Na_i transients (*B*), the rate of sodium/calciumexchange (*C*), and the rate of Ca_i reduction by the CaATPase (*D*) are shown on an expanded time scale (*left*) and on a more prolonged time scale (*right*). The scale bar for time in (*A*) applies to (*A*)–(*D*). In (*E*) and (*F*) the relationship between Ca_i and Na_i for the simulations is shown in (*A*) and (*B*). The thick line is the curve given by Eq. 8. Default parameters were used for simulations.

the exchanger into equilibrium. At this point the Ca-ATPase alone removes calcium, and as it does so it takes the sodium/calcium exchanger out of equilibrium. During the subsequent phase the sodium/calcium exchanger brings calcium into the terminal (Fig. 12 *B*). Plots of Ca_i vs Na_i are altered by including the Ca-ATPase, compared to when only the sodium/calcium exchanger is present (Fig. 12, *E* and *F*). Due to the presence of the calcium ATPase, Ca_i does not plateau at the intersection of the curves defined by Eqs. 5 and 6. Calcium rapidly undershoots the curve given by Eq. 6, bringing the exchanger out of equilibrium until Na_i and Ca_i return to resting levels.

Additional simulations were performed to examine the manner in which the buffer capacity, calcium pump density, and sodium/calcium exchanger density influenced Na_i and Ca_i dynamics (data not shown). Elevating the buffer capacity increased the magnitude of the slow component of Ca_i decay. Increasing the Ca-ATPase density did not significantly influence the Ca_i or Na_i transients in the initial second. There were, however, profound effects on the slower components of the Na_i and Ca_i decay. As the maximum calcium pump velocity was increased, the slow component of Ca_i decay became smaller and faster. The decay of Na_i also became faster. Increasing the sodium/calcium exchanger density sped the rapid decay of Ca_i and the corresponding accumulation of Na_i. In addition, reducing the sodium/calcium exchanger density resulted in notable decreases in the amplitude of the slow component of the calcium decay.

DISCUSSION

Taken together, the experimental results in this paper establish that in cerebellar granule cells presynaptic sodium and calcium levels are coupled. The sodium/calcium exchanger is implicated as a mediator of a large source of sodium accumulation and as the primary means of rapid calcium extrusion. Previously unexplained features of calcium transients are readily explained by an interaction of the sodium/calcium exchanger and the Ca-ATPase. The discussion will deal first with model-independent interpretations of the experimental results, and then with the model of sodium and calcium dynamics that was inspired by these experiments.

Sources of Na_i and Ca_i

The fluorometric detection of Na_i and Ca_i within presynaptic terminals provided information about the sources of calcium and sodium (see Methods). Immediately after stimulation there is a rapid increase in Na_i and Ca_i. Previous studies established that Ca_i increases are a consequence of calcium entry through a variety of voltage-gated calcium channels, with no contribution from internal calcium stores (Mintz et al., 1995; Sabatini and Regehr, 1995). The initial component of Na_i accumulation also occurs very rapidly and is likely a consequence of sodium entry through voltage-gated channels. This is, however, difficult to establish conclusively in this preparation. Owing to the crucial role of sodium channels in action potentials in the parallel fibers, it is not possible to affect sodium channels without altering the presynaptic voltage waveform. This makes the elimination of sodium entry by TTX difficult to interpret.

Surprisingly, most of the presynaptic sodium entry is dependent on calcium entry into the presynaptic terminal and occurs in the several hundred milliseconds after stimulation. This slow component of sodium entry was eliminated by cadmium, which provides a complete block of most types of calcium channels. Furthermore, there was a one-to-one correspondence between the magnitude of calcium influx and the amplitude of the slow component of sodium entry (Figs. 4–6).

Coupling of Na_i and Ca_i immediately after stimulation

Several lines of evidence suggest that changes in Ca_i and Na_i are intimately linked in the second after stimulation.

First, the decay of Ca_i and the accumulation of Na_i have approximately the same time course. Second, as described above, Na_i accumulation is dependent on calcium entry. Third, the rate of decay of Ca_i is dependent upon the concentration of extracellular sodium. Together, these data establish that immediately after stimulation calcium is extruded by a mechanism that leads to sodium entry into parallel fibers. This exchange of sodium for calcium is likely mediated by the sodium/calcium exchanger.

Coupling of Na_i and Ca_i on long times scales

Na_i and Ca_i are also coupled on longer time scales. This is suggested by the similarity of their time courses of return to resting levels. Over the 1-s to 3-min range after stimulation, Na_i and Ca_i can both be approximated by double exponential decays with similar time constants. For the rapid component the time constants of decay are 6–7 s for Ca_i compared to 6–17 s for Na_i. The blockade of calcium influx with cadmium eliminated this component of sodium decay, suggesting that during this phase sodium extrusion was calcium-dependent and involved the sodium/calcium exchanger.

On yet longer time scales, the coupling between calcium and sodium is less clear. There is still a similarity in the time constants of decay over this range, 1–2 min for calcium compared to 2–3 min for sodium. Cadmium did not, however, eliminate the slowest component of Na_i decay. This suggests that the sodium/calcium exchanger may not be a significant factor in sodium removal on these time scales. The sodium/potassium ATPase is an obvious candidate extrusion pathway that may be responsible for Na_i extrusion on long time scales, but this remains to be tested in future studies.

Model of presynaptic Na_i and Ca_i dynamics

A model was constructed that accounted for many features of Na_i and Ca_i dynamics and the coupling of these two ions. The essence of this model is presented schematically in Fig. 13. The presynaptic terminal is shown 4 times, corresponding to the phases of calcium and sodium entry and extrusion shown in the graph: 1) an action potential invades the presynaptic bouton and calcium and sodium enter the presynaptic terminal through voltage-gated channels; 2) sodium/calcium exchanger rapidly removes calcium and brings sodium into the presynaptic fibers; the CaATPase also removes calcium, but at a slower rate than the exchanger; 3) the sodium/calcium exchanger is in equilibrium and there is no net ion flow through the exchanger; and 4) there is a net slow removal of calcium and sodium as the Ca-ATPase removes calcium, but is opposed by the sodium/calcium exchanger.

This model provided good agreement with many features of the measured Na_i and Ca_i transients. First, the coupling of sodium and calcium immediately after stimulation is a consequence of the sodium/calcium exchanger removing calcium in exchange for sodium. Second, there is a transition to a slower decay phase of calcium due to Na_i buildup, which prevents the sodium/calcium exchanger from returning Ca_i all the way to resting levels. Third, this model accounts for the observation that the decay time of calcium from a given level is slower as the number of stimulus pulses in a train is increased. Fourth, this model is consistent with the observed effects of low Na_e on Ca_i transients. Low Na_e should reduce the ability of the sodium/calcium exchanger to remove calcium without greatly affecting its ability to remove sodium. Therefore, according to the model, low Na_e should only slow the most rapid component of Ca_i decay where the sodium/calcium exchanger contributes to calcium extrusion, as was observed experimentally.

This model of presynaptic Na_i and Ca_i dynamics will need to be refined to fully describe Na_i and Ca_i dynamics. Clearly another sodium extrusion mechanism would be required, such as the sodium/potassium ATPase, to account for the decay of sodium at long times after stimulation. Furthermore, more elaborate models of the sodium/calcium exchanger based on the properties of the exchanger in presynaptic terminals [as opposed to the better-characterized cardiac exchanger (Hilgemann, 1988; Hilgemann et al., 1992; Matsuoka and Hilgemann, 1992; Philipson and Nicoll, 1992)] will be needed to capture the subtleties of this

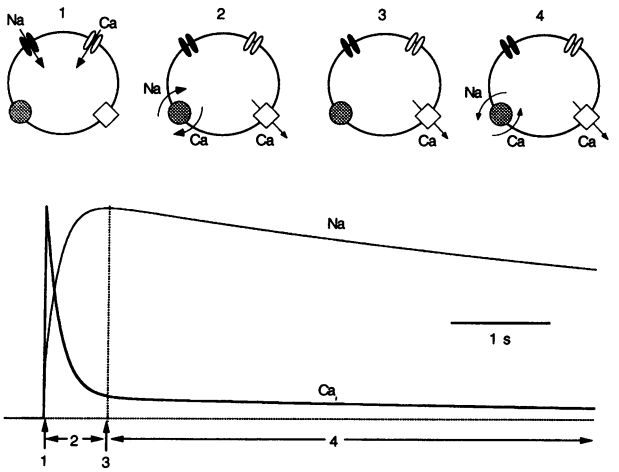

FIGURE 13 Different phases of presynaptic Na_i and Ca_i dynamics. Schematic representation of the response of a presynaptic terminal to stimulation. The presynaptic terminal contains voltage-gated sodium channels (*black*), voltage-gated calcium channels (*white*), a sodium calcium exchanger (*filled circle*), and a calcium ATPase (*square*). The various stages indicated schematically correspond to the times indicated below the graph of presynaptic Na_i and Ca_i. 1) In response to stimulation, sodium and calcium enter through voltage-gated channels. 2) Calcium is removed by both the sodium/calcium exchanger and the Ca-ATPase. During this stage most of the calcium efflux is through the exchanger, which also brings sodium into the presynaptic bouton. 3) The sodium/calcium exchanger reaches steady-state. At this point there is no net ion flow through the exchanger and the Ca-ATPase alone removes calcium. 4) The Ca-ATPase continues to remove calcium from the presynaptic terminal. As it does so the sodium/calcium exchanger is no longer in steady-state and it transports calcium into the bouton and removes sodium.

extrusion system. In addition, this model ignores internal stores of calcium. Even though we have found no evidence for the participation of such stores in calcium signaling for the conditions of our experiments, it is difficult to completely rule out the participation of mitochondria. It is remarkable that even without these refinements the interplay between the sodium/calcium exchanger and the Ca-ATPase can account for so many aspects of sodium and calcium signaling in these terminals.

Implications for Ca_i-dependent synaptic plasticity

These findings have important implications for Ca_i-dependent synaptic plasticity. The rapidly decaying phase of Ca_i after stimulation is responsible for facilitation of transmission at this synapse (Atluri and Regehr, 1996). It appears that the sodium/calcium exchanger is the dominant Ca_i extrusion mechanism on time scales that are relevant to facilitation. The slower decay phase of Ca_i produced by stimulus trains such as those used here ($\tau \approx 5$–20 s), which results from the interaction between the sodium/calcium exchanger and the Ca-ATPase, appears to lead to longer lasting forms of enhancement at this synapse corresponding to posttetanic potentiation (Peters and Regehr, unpublished observations).

It will be interesting to determine whether the interplay between Na_i and Ca_i, observed here in granule cell presynaptic terminals, plays an important role in controlling presynaptic Ca_i dynamics and Ca_i-dependent plasticity at other synapses. Ca_i in other presynaptic terminals has complex kinetics similar in many ways to those described here for granule cell presynaptic terminals (Delaney and Tank, 1994; Delaney et al., 1989; Kamiya and Zucker, 1994; Mulkey and Zucker, 1992; Regehr et al., 1994; Zucker et al., 1994). However, with so many factors involved in calcium regulation it seems likely that complexities in presynaptic calcium dynamics in these terminals might arise in many ways. At the crayfish neuromuscular junction, for example, a buildup of Na_i (Delaney and Tank, 1994; Mulkey and Zucker, 1992) and mitochondrial calcium (Tang and Zucker, 1997) both contribute to a slow decay of calcium that produces PTP. Thus it seems likely that the relative importance of an interplay between sodium and calcium in dictating presynaptic calcium levels will be very much dependent on the type of presynaptic terminal and a variety of factors, including the density of voltage-gated sodium and calcium channels; the capacity of presynaptic terminals to buffer calcium; the density of extrusion mechanisms, and the surface-to-volume ratio of the presynaptic boutons.

I thank P. Atluri, C. Chen, J. Dittman, B. Peters, and B. Sabatini for comments on the manuscript.

This work was supported by National Institutes of Health Grant R01-NS32405–01, a McKnight Scholars Award, and a Klingenstein Fellowship Award in the Neurosciences.

REFERENCES

Allen, T. J. A., D. Noble, and H. Reuter. 1989. Sodium-Calcium Exchange. Oxford University Press, Oxford, 332.

Atluri, P. P., and W. G. Regehr. 1996. Determinants of the time course of facilitation at the granule cell to Purkinje cell synapse. *J. Neurosci.* 16:5661–5671.

Blaustein, M. P. 1988. Calcium transport and buffering in neurons. *Trends Neurosci.* 11:438–443.

Blaustein, M. P., and C. J. Oborn. 1975. The influence of sodium on calcium fluxes in pinched-off nerve terminals in vitro. *J. Physiol.* 247: 657–686.

Blaustein, M. P., and E. M. Santiago. 1977. Effects of internal and external cations and of ATP on sodium calcium and calcium-calcium exchange in squid axons. *Biophys. J.* 20:79–111.

Bouron, A., and H. Reuter. 1996. A role of intracellular Na+ in the regulation of synaptic transmission and turnover of the vesicular pool in cultured hippocampal cells. *Neuron.* 17:969–978.

Carafoli, E., E. Garcia-Martin, and D. Guerini. 1996. The plasma membrane calcium pump: recent developments and future perspectives. *Experientia.* 52:1091–100.

Delaney, K. R., and D. W. Tank. 1994. A quantitative measurement of the dependence of short-term synaptic enhancement on presynaptic residual calcium. *J. Neurosci.* 14:5885–5902.

Delaney, K. R., R. S. Zucker, and D. W. Tank. 1989. Calcium in motor nerve terminals associated with posttetanic potentiation. *J. Neurosci.* 9:3558–3567.

Delbono, O., and E. Stefani. 1993. Calcium transients in single mammalian skeletal muscle fibers. *J. Physiol.* 463:689–707.

Duarte, C. B., C. A. M. Carvalho, I. L. Ferreira, and A. P. Carvalho. 1991. Synaptosomal $[Ca^{2+}]_i$ as influenced by Na^+/Ca^{2+} exchange and K^+ depolarization. *Cell Calcium.* 12:623–633.

Ehrlich, B. E., E. Kaftan, S. Bezprozvannaya, and I. Bezprozvanny. 1994. The pharmacology of intracellular Ca^{2+}-release channels. *Trends Pharmacol. Sci.* 15:145–149.

Feller, M. B., K. R. Delaney, and D. W. Tank. 1996. Presynaptic calcium dynamics at the frog retinotectal synapse. *J. Neurophysiol.* 76:381–400.

Fontana, G., and M. P. Blaustein. 1993. Calcium buffering and free Ca^{2+} in rat brain synaptosomes. *J. Neurochem.* 60:843–850.

Fontana, G., R. S. Rogowski, and M. P. Blaustein. 1995. Kinetic properties of the sodium-calcium exchanger in rat brain synaptosomes. *J. Physiol.* 485:349–364.

Fujii, J. T., F. T. Su, D. J. Woodbury, M. Kurpakus, X. J. Hu, and R. Pourcho. 1996. Plasma membrane calcium ATPase in synaptic terminals of chick Edinger-Westphal neurons. *Brain Res.* 734:193–202.

Fujita, Y., M. Mynlieff, R. T. Dirksen, M.-S. Kim, T. Niidome, J. Nakai, T. Friedrich, N. Iwabe, T. Miyata, T. Furuichi, D. Furutama, K. Mikoshiba, Y. Mori, and K. G. Beam. 1993. Primary structure and functional expression of the ω-conotoxin sensitive N-type calcium channel from rabbit brain. *Neuron.* 10:585–598.

Gill, D. L., E. F. Grollman, and L. D. Kohn. 1981. Calcium transport mechanism in membrane vesicles from guinea pig brain synaptosomes. *J. Biol. Chem.* 256:184–192.

Grynkiewicz, G., M. Poenie, and R. Y. Tsien. 1985. A new generation of Ca^{2+} indicators with greatly improved fluorescence properties. *J. Biol. Chem.* 260:3440–3450.

Harootunian, A. T., J. P. Y. Kao, B. K. Eckert, and R. Y. Tsien. 1989. Fluorescence ratio imaging of cytosolic free Na^+ in individual fibroblasts and lymphocytes. *J. Biol. Chem.* 264:19458–19467.

Helmchen, F., J. G. G. Borst, and B. Sakmann. 1997. Calcium dynamics associated with a single action potential in a CNS presynaptic terminal. *Biophys. J.* 72:1458–1471.

Herrington, J., and R. J. Bookman. 1995. Pulse Control V4.5: IGOR XOPs for Patch Clamp Data Acquisition. University of Miami, Miami, FL.

Hilgemann, D. W. 1988. Numerical approximations of sodium-calcium exchange. *Prog. Biophys. Mol. Biol.* 51:1–45.

Hilgemann, D. W., S. Matsuoka, G. A. Nagel, and A. Collins. 1992. Steady-state and dynamic properties of cardiac sodium-calcium exchange: sodium-dependent inactivation. *J. Gen. Physiol.* 100: 905–932.

Kamiya, H., and R. S. Zucker. 1994. Residual Ca^{2+} and short-term synaptic plasticity. *Nature*. 371:603–606.

Kobayashi, K., and M. Tachibana. 1995. Ca^{2+} regulation in the presynaptic terminals of goldfish retinal bipolar cells. *J. Physiol.* 483:79–94.

Levi, A. J., C. O. Lee, and P. Brooksby. 1994. Properties of the fluorescent sodium indicator "SBFI" in rat and rabbit cardiac myocytes. *J. Cardiovasc. Electrophysiol.* 5:241–257.

Llano, I., A. Marty, C. M. Armstrong, and A. Konnerth. 1991. Synaptic- and agonist-induced excitatory currents of Purkinje cells in rat cerebellar slices. *J. Physiol.* 434:183–213.

Luther, P. W., R. K. Yip, R. J. Bloch, A. Ambesi, G. E. Lindenmayer, and M. P. Blaustein. 1992. Presynaptic localization of sodium/calcium exchangers in neuromusclar preparations. *J. Neurosci.* 12:4898–4904.

Matsuoka, S., and D. W. Hilgemann. 1992. Steady-state and dynamic properties of cardiac sodium-calcium exchange. *J. Gen. Physiol.* 100: 963–1001.

Minta, A., and R. Y. Tsien. 1989. Fluorescent indicators for cytosolic sodium. *J. Biol. Chem.* 264:19449–19457.

Mintz, I. M., B. L. Sabatini, and W. G. Regehr. 1995. Calcium control of transmitter release at a cerebellar synapse. *Neuron*. 15:675–688.

Mintz, I. M., V. J. Venema, K. M. Swiderek, T. D. Lee, B. P. Bean, and M. E. Adams. 1992. P-type calcium channels blocked by the spider toxin ω-Aga-IVA. *Nature*. 355:827–829.

Mulkey, R. M., and R. S. Zucker. 1992. Posttetanic potentiation at the crayfish neuromuscular junction is dependent on both intracellular calcium and sodium ion accumulation. *J. Neurosci.* 12:4327–4336.

Mullins, L. J. 1977. A mechanism for sodium/calcium transport. *J. Gen. Physiol.* 70:681–695.

Neher, E., and G. J. Augustine. 1992. Calcium gradients and buffers in bovine chromaffin cells. *J. Physiol.* 450:273–301.

Palay, S. L., and V. Chan-Palay. 1974. Cerebellar Cortex. Springer-Verlag, New York.

Peng, Y. 1996. Ryanodine-sensitive component of calcium transients evoked by nerve firing at presynaptic nerve terminals. *J. Neurosci.* 16:6703–6712.

Philipson, K. D., and D. A. Nicoll. 1992. Sodium-calcium exchange. *Curr. Opin. Cell Biol.* 4:678–683.

Regehr, W. G., and P. P. Atluri. 1995. Calcium transients in cerebellar granule cell presynaptic terminals. *Biophys. J.* 68:2156–2170.

Regehr, W. G., K. R. Delaney, and D. W. Tank. 1994. The role of presynaptic calcium in short-term enhancement at the hippocampal mossy fiber synapse. *J. Neurosci.* 14:523–537.

Regehr, W. G., and I. M. Mintz. 1994. Participation of multiple calcium channel types in transmission at single climbing fiber to Purkinje cell synapses. *Neuron*. 12:605–613.

Regehr, W. G., and D. W. Tank. 1991. Selective fura-2 loading of presynaptic terminals and nerve cell processes by local perfusion in mammalian brain slice. *J. Neurosci. Meth.* 37:111–119.

Reuter, H., and H. Porzig. 1995. Localization and functional significance of the Na^+/Ca^{2+} exchanger in presynaptic boutons of hippocampal cells in culture. *Neuron*. 15:1077–1084.

Rizzuto, R., C. Bastianutto, M. Brini, M. Murgia, and T. Pozzan. 1994. Mitochondrial Ca^{2+} homeostasis in intact cells. *J. Cell Biol.* 126: 1183–1194.

Rizzuto, R., A. W. Simpson, M. Brini, and T. Pozzan. 1992. Rapid changes of mitochondrial Ca^{2+} revealed by specifically targeted recombinant aequorin. *Nature*. 358:325–327.

Roberts, W. M., R. A. Jacobs, and A. J. Hudspeth. 1990. Colocalization of ion channels involved in frequency selectivity and synaptic transmission at presynaptic active zones of hair cells. *J. Neurosci.* 10:3664–3684.

Rose, C., and B. R. Ransom. 1997. Regulation of intracellular sodium in cultured rat hippocampal neurones. *J. Physiol.* 499:573–587.

Sabatini, B. L., and W. G. Regehr. 1995. Detecting changes in calcium influx which contribute to synaptic modulation in mammalian brain slice. *Neuropharmacology*. 34:1453–1467.

Sanchez-Armass, S., and M. P. Blaustein. 1987. Role of sodium-calcium exchange in regulation of intracellular calcium in nerve terminals. *Am. J. Physiol.* 252:C595–C603.

Satoh, H., H. Hayashi, N. Noda, H. Terada, A. Kobayashi, Y. Yamashita, T. Kawai, M. Hirano, and N. Yamazaki. 1991. Quantification of intracellular free sodium ions by using a new fluorescent indicator, sodium-binding benzofuran isophthalate in guinea pig myocytes. *Biochem. Biophys. Res. Commun.* 175:611–616.

Swandulla, D., M. Hans, K. Zipser, and G. J. Augustine. 1991. Role of residual calcium in synaptic depression and posttetanic potentiation: fast and slow calcium signaling in nerve terminals. *Neuron*. 7:915–926.

Tang, Y., and R. S. Zucker. 1997. Mitochondrial involvement in post-tetanic potentiation of synaptic transmission. *Neuron*. 18:483–491.

Tank, D. W., W. G. Regehr, and K. R. Delaney. 1995. A quantitative analysis of presynaptic calcium dynamics that contribute to short-term enhancement. *J. Neurosci.* 15:7940–7952.

Tucker, T. R., and R. Fettiplace. 1996. Monitoring calcium in turtle hair cells with a calcium-activated potassium channel. *J. Physiol.* 494: 613–626.

Wettwer, E., H. Himmel, and U. Ravens. 1992. Amiloride derivatives as blockers of Na^+/Ca^{2+} exchange: effects on mechanical and electrical function of guinea-pig myocardium. *Pharmacol. Toxicol.* 71:95–102.

Williams, M. E., P. F. Brust, D. H. Feldman, S. Patthi, S. Simerson, A. Maroufi, A. F. McCrue, G. Velicelebi, S. B. Ellis, and M. M. Harpold. 1992. Structure and functional expression of an ω-conotoxin-sensitive human N-type calcium channel. *Science*. 257:389–395.

Zhao, M., S. Hollingworth, and S. M. Baylor. 1996. Properties of tri and tetracarboxylate Ca^{2+} indicators in frog skeletal muscle fibers. *Biophys. J.* 70:896–916.

Zucker, R. S., K. R. Delaney, R. Mulkey, and D. W. Tank. 1991. Presynaptic calcium in transmitter release and posttetanic potentiation. *Ann. N.Y. Acad. Sci.* 635:191–207.